PLASMA LENS EXPERIMENTS AT THE FINAL FOCUS TEST BEAM*

W. BARLETTA[4], S. CHATTOPADHYAY[4], P. CHEN[12], D. CLINE[2],
W. CRADDOCK[12], W. GABELLA[2], I. HSU[9], R. IVERSON[12], T. KATSOULEAS[11],
P. KWOK[2], P. LAI[11], W. LEEMANS[4], R. LIOU[11], D. D. MEYERHOFER[10],
K. NAKAJIMA[8], H. NAKANISHI[8], C. K. NG[12], Y. NISHIDA[13], J. NOREM[1],
A. OGATA[8], S. RAJAGOPALAN[2], T. SHINTAKE[8], J. ROSENZWEIG[2], M. ROSS[12],
A. SESSLER[4], J. SPENCER[12], J. J. SU[7], N. WALKER[12], G. WESTENSKOW[5],
D. WHITTUM[8,12], R. WILLIAMS[3], J. WURTELE[6].

Abstract

We intend to carry out a series of plasma lens experiments at the Final Focus Test Beam facility at SLAC. These experiments will be the first to study the focusing of particle beams by plasma focusing devices in the parameter regime of interest for high energy colliders, and is expected to lead to plasma lens designs capable of unprecedented spot sizes. Plasma focusing of positron beams will be attempted for the first time. We will study the effects of lens aberrations due to various lens imperfections. Several approaches will be applied to create the plasma required including laser ionization and beam induced tunneling ionization of a working gas - the latter which has never been observed before. The compactness of our device should prove to be of interest for applications at the SLC and the next generation linear colliders.

1 INTRODUCTION

Plasma focusing devices are compact, simple, and very strong focusing elements. The focusing strengths for typical parameters are equivalent to ~10^9 Gauss/cm focusing magnets. In principle, such strong fields are capable of focusing beams to very small spot sizes [1-6] and perhaps even capable of avoiding [7] inherent (Oide) limitation [8] in discrete strong focusing. Our goal is to show the effectiveness of plasma lenses in the parameter regime of interest for SLC and the next generation high energy linear colliders. The experience gained is expected to yield new final focus designs capable of producing spot sizes smaller than ever produced before.

There are three low energy, low density beam experimental results which confirm the theory of the beam-plasma interaction performed at ANL [9,10], Tokyo University [11], and

MASTER

UCLA [12]. While such experimental results have been useful, however, the beam densities involved in the ANL, Tokyo, and UCLA experiments were 6 to 7 orders of magnitude lower than the nominal colliding beam density at the SLC and the next generation linear colliders, so that the experience is insufficient to design or evaluate a plasma lens in a high energy collider detector. A beam such as the FFTB offers a unique environment to test all aspects of plasma focusing of high energy, high density, and low emittance beams.

2 PARAMETER STUDIES

When ignoring the effects due to the return current, the focusing strength for underdense plasma lenses is governed by the plasma density n_p,

$$K = \frac{2\pi r_e}{\gamma} n_p \ , \qquad (2.1)$$

whereas for the overdense plasma lenses the strength is determined by the beam density n_b,

$$K = \frac{2\pi r_e}{\gamma} n_b \ . \qquad (2.2)$$

The plasma return current tends to reduce the focusing effect of the lens [13]. The effect is approximately given by

$$K_{rc} = \frac{K}{1 + (k_p \sigma_r)^2} \ , \qquad (2.3)$$

where σ_r is the *rms* size of the beam and $k_p = \sqrt{4\pi r_e n_p}$ is the plasma wavenumber. The effect is appreciable only when the plasma is considerably denser than the beam.

The parameters for plasma lenses in the three density regimes are studied in five cases with round beam and flat beam geometries.

2.1 Round Beam Focusing

In the round beam experiment, the plasma density will be varied to cover all three regimes of the plasma lens from underdense to overdense and to the total compensation limit, at which focusing degrades due to return current. Typical parameters corresponding to these lenses are shown in Table 1.

In the table, ε is the beam energy and ε_n is the normalized emittance. The initial beta at the vacuum waist is β_0^* and s_0 is the beginning of the lens with respect to this waist. The beta function at the entrance to the lens is β_0 and l is the lens thickness. The focal length of the lens is $f = s^* - s_0 - l/2$ where s^* is the distance of the new focal point from the initial one without plasma. The plasma density is n_p and n_{b0} is the peak beam density at the entrance to the plasma.

Beam Parameters	Case 1	Case 2	Case 3
ε [GeV]	50	50	50
N [10^{10}]	1.0	1.0	1.0
ε_n [10^{-5} m-rad]	3.0	3.0	3.0
β_0^* [cm]	7.5	7.5	7.5
σ_{r0}^* [μm]	4.74	4.74	4.74
β_0 [cm]	8.03	8.03	8.03
σ_0 [μm]	4.91	4.91	4.91
σ_z [mm]	0.47	0.47	0.47
n_{b0} [10^{16} cm^{-3}]	5.3	5.3	5.3
Lens Parameters			
n_p [10^{17} cm^{-3}]	0.2	1.0	10
$k_p \sigma_z$	12.5	28.0	88.5
s_0 [cm]	-2.0	-2.0	-2.0
l [cm]	0.3	0.3	0.3
f [cm]	3.80	2.92	3.60
Focused Beam			
β_r^* [mm]	3.7	2.1	3.4
σ_r^* [μm]	3.35	2.55	3.23
s^* [cm]	1.95	1.07	1.75

Table 1: Round Beam Focusing

DISCLAIMER

Portions of this document may be illegible in electronic image products. Images are produced from the best available original document.

2.2 Flat Beam Focusing

With the designed FFTB beam parameters while $N = 2.5 \times 10^{10}$, the beam is intense enough to produce a high density plasma by impact ionization and should even reach the tunneling ionization threshold when close enough to the initial focal point. Theory [6] and simulations [14] of such a scheme suggest substantial plasma focusing. Typical parameters for such plasma lenses are shown in Table 2.

In Case 4, the tunneling ionization threshold is reached right from the start of the lens, and the ionization is quickly saturated. With the complimentary impact ionization, we expect that the plasma so produced should be reasonably uniform, and the aberrations should be much mild. In Case 5, the vertical beam size goes down to ~38 nm, which is about 2/3 of the 60 nm designed FFTB minimum vertical beam size.

Beam Parameters	Case 4	Case 5
ε [GeV]	50	50
N [10^{10}]	2.5	2.5
$\varepsilon_{nx} / \varepsilon_{ny}$ [10^{-5} m-rad]	3.0 / 0.3	3.0 / 0.3
$\beta^*_{x0} / \beta^*_{y0}$ [mm]	3.0 / 3.0	3.0 / 0.12
$\sigma^*_{x0} / \sigma^*_{y0}$ [nm]	1000 / 333	1000 / 60
β_{x0} / β_{y0} [mm]	4.33 / 4.33	4.33 / 33.5
$\sigma_{x0} / \sigma_{y0}$ [nm]	1200 / 400	1200 / 1000
σ_z [mm]	0.47	0.47
n_{b0} [10^{18} cm^{-3}]	7.7	2.8
Lens Parameters		
n_p [10^{18} cm^{-3}]	2.0	2.5
$k_p \sigma_z$	125.1	139.9
s_0 [mm]	-2.0	-2.0
l [mm]	1	1
f [mm]	1.6	1.38 / 0.87
Focused Beam		
β^*_x / β^*_y [mm]	0.9 / 0.9	0.75 / 0.047
σ^*_x / σ^*_y [nm]	520 / 165	480 / 38
s^*_x / s^*_y [mm]	0.10 / 0.10	-0.12 / -0.63

Table 2: Flat Beam Focusing

3 EXPERIMENTAL DESIGNS

3.1 Experimental Setup

The outline of the experiments is shown in Figure 1. The plasma is created in a chamber with ports for ionization laser, plasma diagnostics and beam size measuring devices. A three stage differential pumping system is used to keep the beam line pressure at 10^{-6} torr or better. The setup is to be installed at the FFTB final focus region near Station 1027. An isometric view of the design is shown in Figure 2.
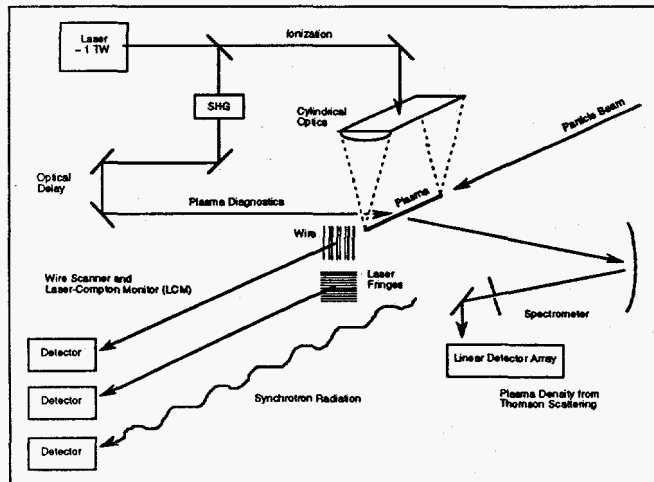

Figure 1: Outline of Plasma Lens Experimental Setup

3.2 Plasma Chamber

The plasma chamber is shown in the center of Figure 2. The chamber has a small pipe with a diameter of 1 or 3 mm inside which runs transversely to the direction of the particle beam. A pressure differential is maintained between the gas connections for a laminar gas flow through the pipe. The particle beam enters the gas pipe and exits through 0.01 cm holes at the center of the chamber. Pumping connections on both sides of the chamber capture most of the gas leakage through the particle beam entrance and exit holes. Ionization, diagnostic, and beam size
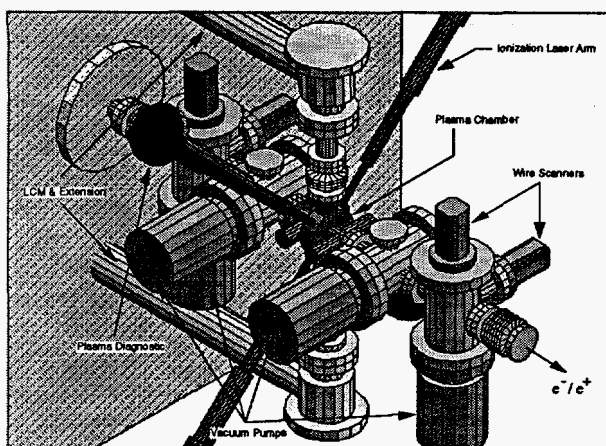
3

Figure 2: Plasma Lens Experiments at the FFTB.

measurement lasers are injected through ports on the perimeter of the chamber that connect to the gas pipe. Hydrogen gas will be used to minimize the background from beam-plasma interaction. Several plasma chambers will be fabricated with adaptations to different phases of the experimental program.

3.3 Vacuum System

For the maximum plasma density in Case 5 of $n_p = 2.5 \times 10^{18}$ cm^{-3}, a H$_2$ pressure of about 39 torr at room temperature is required. In order to keep pumping requirements within a practical range, a three stage differential pumping system is used on both sides of the plasma chamber. Using a 70 liter/sec hybrid turbo molecular pump, the majority of the gas is picked up at a high pressure. The gas then flows through a narrow, high impedance restrictor into the second pumping stage which is pumped through a 9.68 cm (3.8") port by a 210 liter/sec turbo molecular pump to a pressure of 2.7×10^{-5} torr. The remaining gas flows through a second restrictor into the third pumping stage which has identical dimensions and pumping speed as the second stage. A pressure of 3.5×10^{-7} torr can be reached after the third pumping stage. Approximately 1.5×10^{-11} gm/sec flows down the beam line where it is captured by two ion pumps. The dimensions of the restrictors between pumping stages are chosen to have the proper clearances for the particle beam. With the small quantities of hydrogen involved, hydrogen safety for the vacuum system should not be a problem.

3.4 Laser Systems

The ionizing laser pulse for the experiments will be generated from the same 1 μm wavelength laser system which has been developed for the E-144 [15] experiment at the FFTB. The high-powered Nd:glass laser is based on the concept of chirped pulse amplification and compression (CPA) [16-19], which will produce pulses of 1 ps duration with energies up to about 2 J (~2 TW) at 1 Hz. The laser will be synchronized to the electron beam with an accuracy of ~1 ps.

For the plasma lens experiments, a small portion of the laser energy will be splitted off and frequency doubled to provide a 0.5 μm wavelength pulse for plasma diagnostics [20]. The bulk of the energy will be focused with a cylindrical lens to form the plasma lens.

3.5 Beam Size Monitors (BSM)

For the round beams of Case 1, 2, and 3, beam sizes of ~2 - 4 μm are involved. The BSM for these cases is a wire scanner using carbon fibers [21]. Fibers of ~4 μm in diameter should allow the measurement of beam sizes to ~2 μm and sustain beam intensity of 1×10^{10}. The bremsstrahlung yields are measured using existing bremsstrahlung detectors installed for the FFTB wire scanners.

For Case 4 and 5, spot sizes with σ_x at ~0.5 - 1 μm, and σ_y of order 40 nm are involved. The BSM for these cases is a version of the Laser-Compton Monitor (LCM) developed by T. Shintake [22]. Since only Mode 1 and 3 of the monitor [23] are sufficient for Case 4 and 5, the implementation will be simpler than the LCM installed for the FFTB. The required laser is

shared with the FFTB version of the monitor by mechanically inserting a beam splitter/mirror into the existing laser transport line.

In addition, a synchrotron radiation monitoring system is under development as a supplemental beam size measurement method and for the study of plasma beamstrahlung suppression.

3.6 Supersonic Gas Jet

A supersonic gas jet is under development to replace the plasma chamber. The jet will provide a narrow (1 - 3 mm) stream of gas transversing the path of the particle beam at a velocity in excess of 2500 m/s. With the supersonic gas jet approach, potential beam tuning problem through the 100 μm holes of the plasma chamber is eliminated. In fact, the jet can also serve as a beam finder for initial beam tuning.

With the supersonic gas jet the hardware present at the interaction point is minimal, and the background due to the photons accompanying the particle beam interacting with the plasma lens setup will be greatly reduced. The vacuum pumping requirement along the beam line is reduced as most of the gas will enter the collector cone before it can escape into the beam line. A three stage differential pumping system will be used behind the collector cone to remove the gas from the supersonic gas jet.

3.7 Plasma Lens Prototype System

A prototype system of the plasma lens experimental setup has been constructed in July '93. The system is essentially one half of the experimental design as shown in Figure 2, and is highly configurable for testing various components for the plasma lens experiments. Vacuum pumping requirements for the experiments have been successfully verified in Sept. '93 using the system. The system will be reconfigured for the testing of the supersonic gas jet in the Fall of 1994.

3.8 Plasma Production Test

The plasma production test is scheduled to be performed at the Laboratory of Laser Energetics of the University of Rochester in August '94. The test will be performed using a laser system similar to the one installed at the FFTB but firing at a slower repetition rate. The goal will be to demonstrate the production of a plasma with thickness of ~1 mm and density of the order of 10^{18} cm^{-3} for the plasma lens experiments. Testing of plasma production with the supersonic gas jet is scheduled in the Fall of 1994.

4 SUMMARY

The series of experiments to be performed will serve to characterize plasma focusing devices, and if successful, will lead to practical applications at the SLC and the next generation of linear colliders. The primary goal of our experiments is to study the focusing of high energy and high density particle beams by plasma lenses of various densities and thicknesses. Plasma focusing of positron beams will be demonstrated for the first time. With a bunch population of about 2.5×10^{10} from the FFTB, we will demonstrate the tunneling ionization of a gas target by an electron beam, and establish the plasma lens as a simple, compact and economical add-on device for luminosity enhancement in linear colliders. Furthermore, the total compensation of beam self-fields by the plasma can be of interest for beamstrahlung suppression in future linear colliders.

REFERENCES

[1] P. Chen, Part. Accel. **20**, 171 (1987).

[2] P. Chen, J. J. Su, T. Katsouleas, S. Wilks, and J. M. Dawson, IEEE Trans. Plasma Sci. **15**, 218 (1987).

[3] J. B. Rosenzweig and P. Chen, Phys. Rev. D **39**, 2039 (1989).

[4] P. Chen, S. Rajagopalan, and J. B. Rosenzweig, Phys. Rev. D **40**, 923 (1989).

[5] J. J. Su, T. Katsouleas, J. M. Dawson, and R. Fedele, Phys. Rev. A **41**, 3321 (1990).

[6] P. Chen, Phys. Rev. A **45**, R3398 (1992).

[7] P. Chen, K. Oide, A. Sessler, and S. Yu, Phys. Rev. Lett. **64**, 1231 (1990).

[8] K. Oide, Phys. Rev. Lett. **61**, 1713 (1988).

[9] J. B. Rosenzweig *et al.*, Phys. Fluids B **2**, 1376 (1990).

[10] J. B. Rosenzweig *et al.*, Phys. Rev. Lett. **61**, 98 (1988).

[11] H. Nakanishi *et al.*, Phys. Rev. Lett. **66**, 1870 (1991).

[12] G. Hairapetian *et al*, Phys. Rev. Lett. **72**, 2403 (1994).

[13] D. H. Whittum *et al.*, Part. Accel. **34**, 89 (1990).

[14] P. Chen, C. K. Ng, and S. Rajagopalan, Phys. Rev. E **48**, 3022 (1993).

[15] J. G. Heinrich *et al*, "SLAC Proposal E-144," SLAC (1991).

[16] S. Augst, D Strickland, D. D. Meyerhofer, S. L. Chin, and J. H. Eberly, Phys. Rev. Lett. **63**, 2212 (1989).

[17] D. Strickland *et al.*, Opt. Comm. **56**, 219 (1985).

[18] P. Maine, D. Strickland, P. Bado, M. Pessot, and G. Mourou, IEEE J. Ouant. Elec. **24**, 398 (1988).

[19] Y. H. Chuang, D. D. Meyerhofer, S. Augst, H. Chen, J. Peatross, and S. Uchida, J. Opt. Soc. Am B **8**, 1226 (1991).

[20] J. Sheffield, "Plasma Scattering of Electromagnetic Radiation," Academic Press, New York (1975).

[21] C. Field *et al.*, Nuc. Inst. Meth. A **295**, 279 (1990).

[22] T. Shintake, Nuc. Inst. Meth. A **311**, 453 (1992).

[23] T. Shintake *et al.*, KEK Preprint 92-065 (1992).

DISCLAIMER